Texture Measurement and Identification of Object Surface by MEMS Tactile Sensor

Masayuki Sohgawa*, Kosuke Watanabe†, Takeshi Kanashima†,
Masanori Okuyama†, Takashi Abe*, Haruo Noma‡, and Teruaki Azuma§
*Graduate School of Science and Technology, Niigata University, Niigata, Japan 950–2181
Email: sohgawa@eng.niigata-u.ac.jp
†Graduate School of Engineering Science, Osaka University, Toyonaka, Osaka, Japan 560–8531
‡College of Information Science and Engineering, Ritsumeikan University, Kusatsu, Shiga, Japan 525–8577
§Nitta Corporation, Tokyo, Japan 104–0061

***Abstract*—The surface texture of various materials has been characterized by tactile sensor with a micro-cantilever embedded in the PDMS elastomer. The maximum output (resistance of strain gauge on the cantilever) change of the sensor by indentation of the object on the sensor surface depends on the hardness or thickness of the object. Moreover, output change is asymmetric in a back-and-forth indentation test because of relaxation of deformation. On the other hand, the output increases rapidly at beginning of stepwise sliding of the sensor at the object surface because of static friction, and changes periodically corresponding to stick-slip oscillation or surface roughness after slipping. It is demonstrated that about 30 materials of papers, clothes, leathers, and plastic sheets, have been classified into 5 clusters by the principal component analysis using feature quantities extracted from the sensor outputs.**

I. Introduction

Recently, robots with skillful performance comparable with human in nursing care of aged and automation in manufacturing, agriculture, etc. have attracted much attention [1], [2]. To ensure safety and workability for these applications, robots should recognize the work objects by detecting surface texture, including friction, roughness, hardness, and so on. However, current conventional sensors such as optical, sonic and pressure sensors remain insufficient for this purpose [3].

We have proposed a miniature multi-axial tactile sensor which can simultaneously detect normal and shear forces, and measurement method identifying surface texture of the objects by indentation and scanning of the tactile sensor like human active touching [4], [5]. It has been demonstrated that papers with various surface textures such as glossy, smooth, rough, or soft surface, can be classified in 5 clusters by the principal component analysis using the feature quantities extracted from the output of the tactile sensor [6]–[8]. In this work, new categories of the object such as clothes, leathers, and plastics have been added and analyzed by some additional feature quantities.

II. Tactile Sensor for Surface Texture Measurement

A. Structure of the Sensor

Fig. 1 shows a schematic illustration of the tactile sensor with micro-cantilevers for the texture measurement. The micro-cantilever can be deflected by application of both normal and shear forces because of its inclined shape. The deflection of the micro-cantilever is detected as a resistance change of the NiCr strain gauge film. The micro-cantilever is embedded in the elastomer (polydimethylsiloxane; PDMS) for protection of fragile structures and flexibility of a contact site. The elastomer is formed hemispherical shape to reduce the contact area.

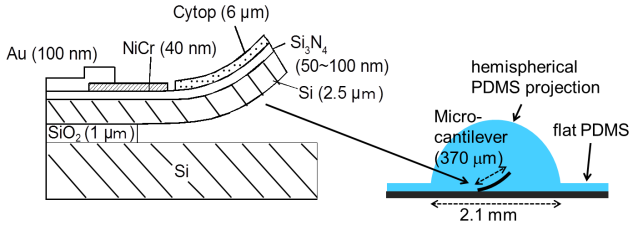

Fig. 1. A schematic illustration of the tactile sensor with the micro-cantilever.

B. Fabrication Process

The micro-cantilever was fabricated by the surface micromachining process. A silicon-on-insulator (SOI) wafer was used as a substrate. Thicknesses of the Si substrate, buried oxide, and thin Si layers are 500, 1, and 2.5 μm, respectively. At first, a Si_3N_4 thin film (thickness: 50 $\sim$ 100 nm) as an insulating layer, a NiCr alloy thin film (thickness: 40 nm) as a detection layer, and a Au layer (thickness: 100 nm) as an electrode were deposited successively by sputtering method. NiCr (Ni:Cr=5:5) thin-film strain gauge has the low temperature coefficient so that the output of the sensor is thermally stable [4]. After wire patterning by photolithography, a Cytop (Asahi Glass) film (thickness: 6 μm) was spin-coated and cured at 200°C for 1 hour in order to bend the cantilever structure upward. After forming etching window by reactive ion etching (RIE), the cantilever structure was formed by the sacrificial etching of the buried oxide layer in buffered hydrofluoric acid (BHF) solution (NH_4HF_2: 20%) for about 6 hours, and then dried in a vacuum after rinsing in ultrapure water and then in ethanol. The Si_3N_4, NiCr, Au, and Cytop films have enough durability against BHF solution for about 6 hours. The etching time is controlled by using etching marker which is peeled off when the micro-cantilever is released from the substrate. The micro-cantilevers were overlaid with PDMS thick film (thickness: tens of μm) by spin-coating, and

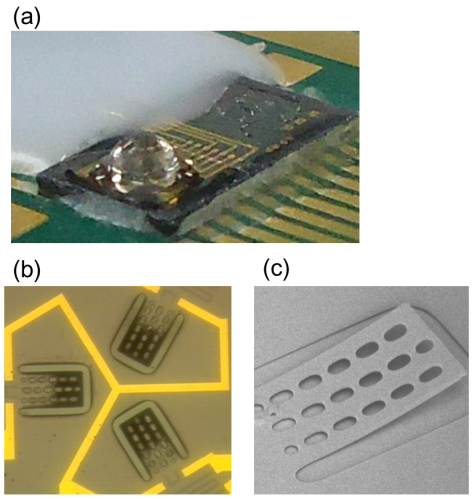

Fig. 2. (a) A photograph of the fabricated tactile sensor with hemispherical PDMS elastomer on a printed circuit board, (b) a microscopic image of 3 cantilevers, and (c) SEM image of a micro-cantilever.

then covered with hemispherical PDMS projection (diameter: about 2.1 mm). The PDMS film and projection were cured at 90°C for 30 min. After mounting the sensor chip on the printed circuit board, they were electrically connected using Au wires. Finally, the Au wire was protected mechanically by using potting resin. Fig. 2(a) shows a photograph of the fabricated tactile sensor mounted on a printed circuit board. The micro-cantilever has an inclined shape as designed, as shown in Figs. 2 (b) and (c).

III. Measurement Method

For texture measurement, the tactile sensor and the object were fixed on the xy horizontal stage and z vertical stage, respectively. The applied force to the sensor surface was monitored by 6-axis force sensor (Nitta, UFS 2012A-05) installed in z stage. Fig. 3 shows the procedures for texture measurement. In the first procedure, as shown in Fig. 3 (a), the object is indented on the sensor surface (top of the PDMS hemispherical projection) to a certain depth (0.2 mm), and then pulled up. In the second procedure, as shown in Fig. 3 (b), the object is contacted to the sensor surface at a constant force, and then slid to the longitudinal direction of the cantilever. The second procedure is a similar measurement to the second one, but the object is slid along the transverse direction to the cantilever, as shown in Fig. 3 (c). The resistance change of the strain gauge on the micro-cantilever during these procedures was measured by the precise digital multimeter (ADMCT, R6581).

IV. Results and Discussion

A. Indentation Measurement

Fig. 4 shows relative resistance changes of the tactile sensor as a function of time by indention and pull-up, as shown in Fig. 3 (a). After adjusting touch force to 5 gf, the object was indented on the sensor surface to 0.2 mm at a speed of 0.5 mm/s, then it was pulled up to initial position at the same speed. The resistance of the strain gauge on the cantilever decreases with indentation and increases with pull-up, respectively, because of the reaction force of the object.

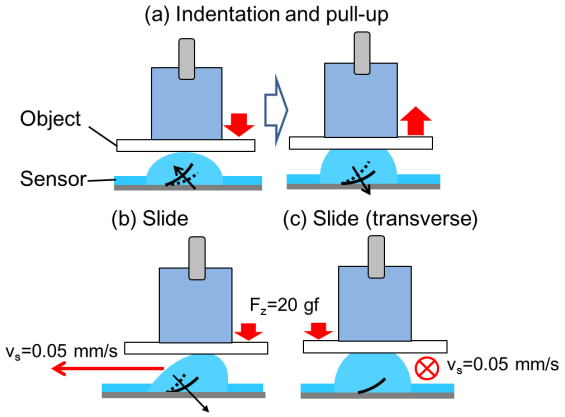

Fig. 3. Texture measurement procedures for active touch sensing, (a) indentation and pull-up, (b) slide, and (c) slide in the transverse direction to the cantilever, respectively.

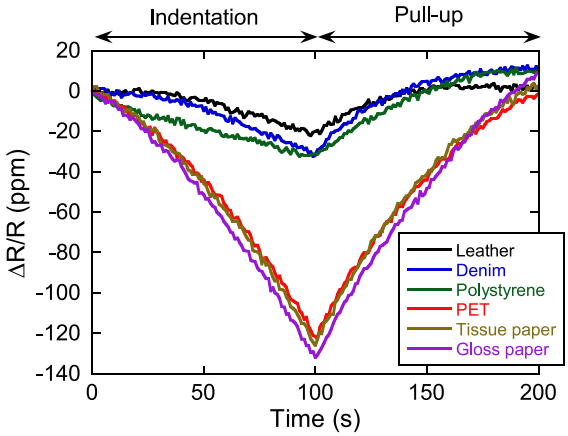

Fig. 4. Relative resistance changes of the tactile sensor as a function of time when the objects are indented on the sensor and then pulled up.

The maximum resistance change (indentation depth: 0.2 mm at 100 s) in Fig. 4 depends on the hardness or thickness of the object. In the case of soft and thick materials such as denim fabric and leather, the maximum resistance change is small because of the small reaction force, by contrast, it is large because of large reaction force in the case of hard and thin materials such as papers and plastic sheets. Moreover, resistance change is asymmetric in indentation and pull-up tests because of relaxation of deformation. As a result, it is found that the maximum resistance change by indentation reflects the hardness and thickness of the object, and time to the initial resistance value reflects the relaxation time of the deformation of the object.

B. Sliding Measurement

Fig. 5 shows relative resistance changes as a function of time when the sensor is slid on the object surface as shown in Fig. 3 (b). After adjusting the normal force to 20 gf, the object was horizontally slid on the sensor surface to the longitudinal direction of the cantilever at 0.05 mm/s after 5 s. The resistance increases drastically after 5 s because of

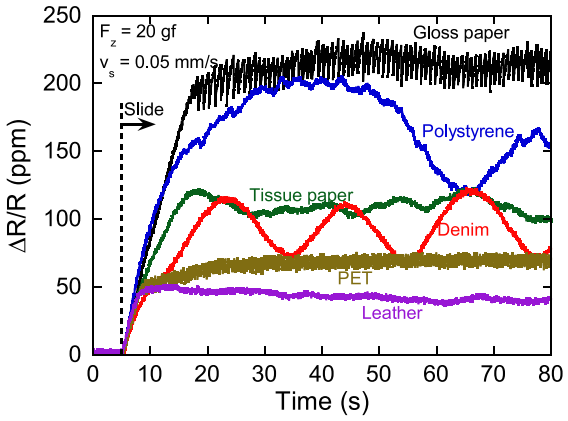

Fig. 5. Relative resistance changes of tactile sensor as a function of time when the sensor is slid on the objects.

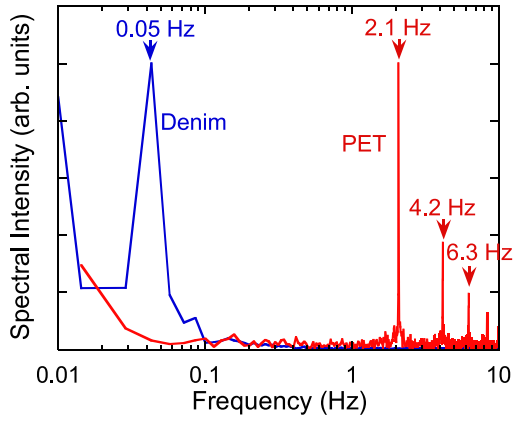

Fig. 6. Frequency spectra of resistance change for denim fabric and PET sheet.

increase of static friction force, and then the object slips on the sensor surface and the resistance changes periodically or gradually caused by surface roughness of the object when shear force exceeds the maximum friction force. For gloss paper and polyethylene terephthalate (PET), the resistances after slipping change short-periodically. Fig. 6 shows frequency spectra of the resistance change for denim fabric and PET sheet obtained by the fast Fourier transformation (FFT) technique. In the case of denim fabric, only one peak appears at 0.05 Hz. Time period corresponding to this peak is 20 s, so that spatial period is 1 mm because of a speed of 0.05 mm/s, which well agrees with distance between the yarns of denim fabric observed with a microscope. By contrast, in the case of PET sheet, there are a fundamental peak at 2.1 Hz with high-order peaks at integral multiples of the fundamental frequency. It is considered that the resistance change for PET sheet is a sawtooth waveform typically caused by stick-slip oscillation [9].

On the other hand, for sliding in the transverse direction as shown if Fig. 3 (c), only long-periodic changes corresponding to surface roughness are observed as shown in Fig 7, because the micro-cantilever is hardly deflected in lateral direction. As a result, it is found that the resistance increase before slipping reflects the static friction coefficient of the object, and amplitude and period of the resistance change after slipping

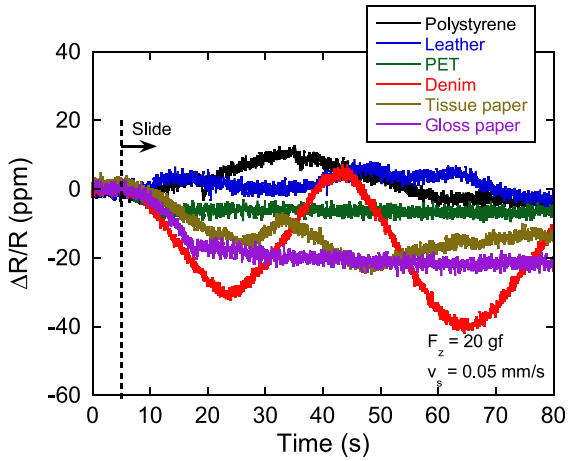

Fig. 7. Relative resistance changes of tactile sensor as a function of time when the sensor is slid on the objects in transverse direction.

TABLE I. DEFINITION OF FEATURE QUANTITIES

Feature quantity	Definition
A	The maximum resistance change by indentation (Fig. 4)
B	Relaxation time to initial resistance value (Fig. 4)
C	Resistance change before slipping (Fig. 5)
D	Standard deviation of resistance change after slipping (Fig. 5)
E	Fundamental frequency of periodically resistance change (Fig. 6)
F	Resistance change after stopping [7], [8]
G	Standard deviation of resistance change after slipping (transverse direction) (Fig. 7)

reflect surface roughness or stick-slip oscillation.

C. Principal Component Analysis

We have extracted 7 feature quantities (listed up in Table I) of the resistance change as shown in Figs. 4–7, such as the maximum change by indentation, frequency of periodically change at slipping. The feature quantities have been analyzed by the principal component analysis (PCA). PCA is one of the multivariate analyses to convert a set of observations of correlated variables into a set of values of linearly uncorrelated variables called principal components. Table II shows the correlation matrix among feature quantities for 32 materials, including papers, cloths, leathers, plastics, and so on. The principal scores are obtained from the eigenvalue and eigenvector of the correlation matrix. Figs. 8–10 show principal score mappings, where the cumulative contribution ratio of from the first to third principal components is 80%. The objects can be classified in 5 clusters which have a similar surface texture by the hierarchical clustering analysis using Ward's method [10], as shown by circles in Fig. 10. It seems that the first principal component may include information of "bulky (vs. sleasy) feeling" because its score is positive value for wipes and clothes (paper towel, polystyrene foam, denim fabric, etc.) and negative value for standard (thin) papers and plastics (PET, PVC, etc.). On the other hand, the second and third principal components seem to indicate "inelastic (vs. elastic) feeling" and "slippery (vs. grippy) feeling", respectively.

V. CONCLUSION

The tactile sensor with micro-cantilevers embedded in the hemispherical elastomer has been fabricated and characterized

TABLE II. CORRELATION MATRIX AMONG FEATURE QUANTITIES

	A	B	C	D	E	F	G
A	1	0.93	0.41	−0.37	0.24	−0.08	−0.41
B	0.93	1	0.39	−0.22	0.25	0.11	−0.23
C	0.41	0.39	1	0.32	−0.06	−0.03	0.03
D	−0.37	−0.22	0.32	1	−0.31	0.51	0.66
E	0.24	0.25	−0.06	−0.31	1	−0.3	−0.3
F	−0.08	0.11	−0.03	0.51	−0.3	1	0.52
G	−0.41	−0.23	0.03	0.66	−0.3	0.52	1

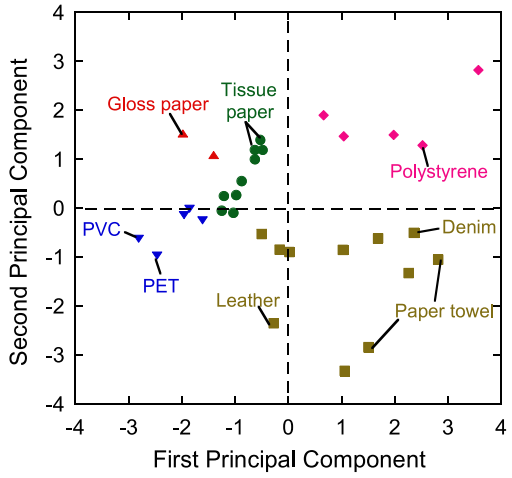

Fig. 8. Principal component mapping of various objects for the first and second principal components.

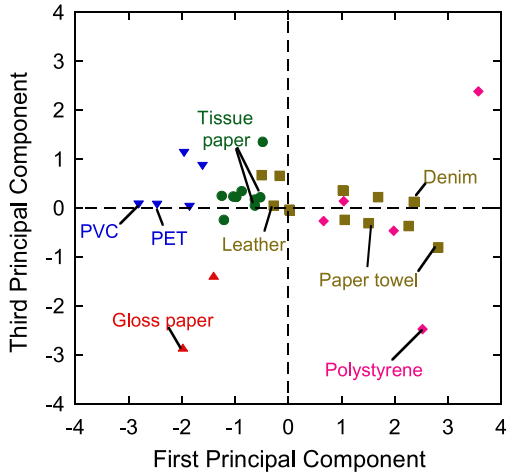

Fig. 9. Principal component mapping of various objects for the first and third principal components.

in indentation and sliding tests for detection of surface texture of the object. Sensor output (resistance change of strain gauge on the micro-cantilever) reflecting surface texture such as hardness, friction, roughness, etc., can be measured by indentation and sliding of the object on the tactile sensor surface. From the sensor outputs, 7 feature quantities have been extracted, and the principal component analysis has been performed by using feature quantities. Consequently, it is found that the first, second, and third principle component obtained by PCA indicate "bulky", "inelastic", and "slippery" feelings of the object, respectively. The 32 objects can be classified in 5 clusters by the hierarchical clustering analysis of PCA score

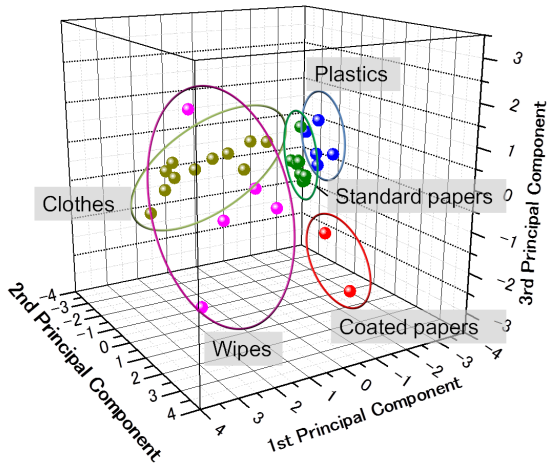

Fig. 10. 3-dimensional principal component mapping of various objects.

obtained from output of the fabricated tactile sensor. Therefore, it is expected that quantitative data of complex surface texture of work objects obtained from the proposed tactile sensor allows for exquisite control of robots.

REFERENCES

[1] T. Mukai, S. Hirano, H. Nakashima, Y. Sakaida, and S. Guo, "Realization and Safety Measures of Patient Transfer by Nursing-Care Assistant Robot RIBA with Tactile Sensors," J. Robot. Mechatronics, vol. 23, no. 3, pp. 360–369, 2011.

[2] M. I. Tiwana, S. J. Redmond, and N. H. Lovell, "A review of tactile sensing technologies with applications in biomedical engineering," Sensors Actuators A Phys., vol. 179, pp. 17–31, 2012.

[3] R. S. Dahiya, G. Metta, M. Valle, and G. Sandini, "Tactile Sensing–From Humans to Humanoids," IEEE Trans. Robot., vol. 26, no. 1, pp. 1–20, 2010.

[4] M. Sohgawa, D. Hirashima, Y. Moriguchi, T. Uematsu, W. Mito, T. Kanashima, M. Okuyama, and H. Noma, "Tactile sensor array using microcantilever with nickel-chromium alloy thin film of low temperature coefficient of resistance and its application to slippage detection," Sensors Actuators A Phys., vol.186, pp. 32–37, 2012.

[5] H. Yokoyama, T. Kanashima, M. Okuyama, T. Abe, H. Noma, T. Azuma, and M. Sohgawa, "Active Touch Sensing by Multi-axial Force Measurement Using High-Resolution Tactile Sensor with Microcantilevers," IEEJ Trans. Sensors Micromachines, vol.134, pp.58–63, 2014.

[6] M. Sohgawa, K. Watanabe, T. Kanashima, M. Okuyama, H. Noma, and T. Azuma, "Review of Texture Measurement of Object Surface by Tactile Sensor with Inclined Micro-cantilevers," IEEJ Trans. Sensors Micromachines, vol. 133, no. 5, pp. 147–154, 2013.

[7] K. Watanabe, M. Sohgawa, T. Kanashima, M. Okuyama, and H. Nona, "Identification of various kinds of papers using multi-axial tactile sensor with micro-cantilevers," in 2013 World Haptics Conference (WHC), 2013, pp. 139–144.

[8] K. Watanabe, M. Sohgawa, T. Kanashima, M. Okuyama, H. Noma, and T. Azuma, "Multi-axial tactile sensor with micro-cantilever embedded in hemispherical elastomer for surface texture measurement," in 2013 Transducers & Eurosensors XXVII: The 17th International Conference on Solid-State Sensors, Actuators and Microsystems, 2013, June, pp. 1012–1015.

[9] S. Maegawa and K. Nakano, "Mechanism of stick-slip associated with Schallamach waves," Wear, vol. 268, no. 7–8, pp. 924–930, 2010.

[10] J. H. Ward, "Hierarchical Grouping to Optimize an Objective Function," J. Am. Stat. Assoc., vol. 58, no. 301, pp. 236–244, 1963.